

# Structure and properties of a novel fulleride $Sm_6C_{60}$

X. H. Chen, Z. S. Liu and S. Y. Li

*Structural Research Laboratory and Department of Physics, University of Science and Technology of China, Hefei, Anhui 230026, P. R. China*

H. C. Dam, and Y. Iwasa

*Japan Advanced Institute of Science and Technology  
Tatsunokuchi, Ishikawa 923-1292, Japan*

(March 12, 1999)

## Abstract

A novel fulleride  $Sm_6C_{60}$  has been synthesized using high temperature solid state reaction. The Rietveld refinement on high resolution synchrotron X-ray powder diffraction data shows that  $Sm_6C_{60}$  is isostructural with body-centered cubic  $A_6C_{60}$  (A=K, Ba). Raman spectrum of  $Sm_6C_{60}$  is similar to that of  $Ba_6C_{60}$ , and the frequencies of two  $A_g$  modes in  $Sm_6C_{60}$  are nearly the same as that of  $Ba_6C_{60}$ , suggesting that Sm is divalent and hybridization between  $C_{60}$  molecules and the Sm atom could exist in  $Sm_6C_{60}$ . Resistivity measurement shows a weak T-linear behavior above 180 K, the transport at low temperature is mainly dominated by granular-metal theory.

**PACS numbers: 71.20.Tx, 78.30.-j, 67.57.Hi**

Alkali intercalation into the  $C_{60}$  host lattice is a successful technique for synthesizing new fullerides.<sup>1</sup> Hereafter, an extensive research has been concentrated on the intercalation of a wide variety of atoms or molecules in the  $C_{60}$  solids. Intercalation of alkali metals in the  $C_{60}$  solids yields various structural compounds  $A_xC_{60}$  (x=1, 3, 4, 6) with different physical property.<sup>2-6</sup> Among these, the superconducting compounds,  $A_3C_{60}$ , has attracted considerable interest.<sup>3</sup> In this system, the fcc lattice parameter and band filling are tunable by changing the intercalants,  $T_c$  goes up with increasing lattice parameter,<sup>7</sup> while it rapidly decreases when the nominal valence ( n ) shifts from the half-filling n=3 of  $t_{1u}$  band.<sup>8</sup>

The study was then extended to the alkali-earth series of  $AE_xC_{60}$ ,<sup>9-12</sup> the electrons are introduced by intercalation of alkali-earth metals into the next lowest unoccupied molecular orbital with  $t_{1g}$  symmetry. The superconducting compounds with various structures and critical temperatures were prepared ( $Ca_5C_{60}$ ,  $Ba_4C_{60}$ ,  $Sr_4C_{60}$ ).<sup>9,13</sup> Such tolerance for the  $C_{60}$  molecular valence in  $t_{1g}$  superconductors makes a striking contrast with the strict constraint for the valence state in the case of  $t_{1u}$  superconductors.

The rare-earth metals were also intercalated into the  $C_{60}$  solids, but only one phase  $RE_{2.75}C_{60}$  (RE=Yb, Sm) was discovered so far.<sup>14,15</sup> In this system, the basic structure of

$RE_{2.75}C_{60}$  is face-centered cubic, but the cation vacancy ordering in tetrahedral sites leads to a superstructure accompanied with slight lattice deformation from cubic to orthorhombic. The RE cations occupying the octahedral sites experience off-center displacements since one out of every eight tetrahedral sites in the subcell is vacant. Such vacancy-ordered structure of  $RE_{2.75}C_{60}$  can be understood within a simple electrostatic energy model.<sup>16</sup> In this paper, we report synthesis and structure of a novel Sm-intercalated compound  $Sm_6C_{60}$ , which is isostructural with bcc  $A_6C_{60}$  (A=K, Ba).<sup>6,10</sup> It suggests that the cation vacancy ordering could not exist in the highly doped  $C_{60}$  with rare earth metals. Raman scattering indicates that the positions of the two  $A_g$  modes in  $Sm_6C_{60}$  are the same as that of  $Ba_6C_{60}$ , suggesting that the Sm is divalent and hybridization between  $C_{60}$  and Sm atoms could exist in  $Sm_6C_{60}$ . The highly Sm-doped  $Sm_6C_{60}$  was confirmed to be metallic by resistivity measurement.

Samples of  $Sm_6C_{60}$  was synthesized by reacting stoichiometric amount of powers of Sm and  $C_{60}$ . A quartz tube with mixed powder inside was sealed under high vacuum of about  $2 \times 10^{-6}$  torr. The sample of  $Sm_6C_{60}$  were calcined at 550 °C for 216 hours with intermediate grindings of two times. X-ray diffraction(XRD) measurements were carried out with synchrotron radiation at the photon Factory of the National Laboratory for High Energy Physics (KEK-PF, Tsukuba). The synchrotron beam was monochromatized to 0.8500 Å. Rietveld refinements for the XRD patterns were carried out using Fullprof-98. X-ray diffraction showed that all samples were single phase, which is also confirmed by the single peak feature of the pentagonal pinch  $A_g(2)$  mode in the Raman spectra.

Raman scattering experiments were carried out using the 632.8 nm line of a He-Ne laser in the Brewster angle backscattering geometry. The scattering light was detected with a Dilor xy multichannel spectrometer using a spectral resolution of  $3 \text{ cm}^{-1}$ . In order to obtain good Raman spectra, the samples were ground and pressed into pellets with pressure of about  $20 \text{ kg/cm}^2$ , which were sealed in Pyrex tubes under a high vacuum of  $10^{-6}$  torr.

Resistivity measurements were carried out using four-probe method. Electrical contacts of less than  $2 \text{ } \Omega$  resistance were established by silver paste. Preparation of samples and electrical contacts was carried out in a controlled argon glove box where the oxygen and water vapor levels were maintained below a few parts per million.

Figure 1 shows the XRD pattern of the  $Sm_6C_{60}$  sample. The pattern is similar to that for the well-known bcc structure found in  $A_6C_{60}$  (A=K, Rb, Cs, and Ba).<sup>6,10</sup> All the observed peaks are indexed with bcc lattice of  $a=10.890 \text{ } \text{Å}$ . The diffraction pattern of  $Sm_6C_{60}$  samples fits well to a single body-centered cubic structure. We have carried out a Rietveld refinement of the structure using the Fullprof-98. The solid line in Fig.1 shows fitted data to a model of the bcc structure (space group  $I_{m\bar{3}}$ ). Refinement of 220 peaks yielded an intensity R factor of  $R_{wp}=9.9\%$  and  $R_p=9.4\%$ , and the following coordinates: C1 at 0.0660, 0.0, 0.3201; C2 at 0.1320, 0.1070, 0.2796; C3 at 0.0660, 0.2140, 0.2392; and Sm at 0.0, 0.5, 0.2749. Mean-square thermal amplitudes of the isotropic Debye-Waller factors were refined to 0.016 and  $0.103 \text{ } \text{Å}^2$  for C and Sm, respectively, and all samarium sites were found to be occupied. The refined lattice constant,  $a=10.890 \text{ } \text{Å}$ , however, is significantly smaller than measured values for  $K_6C_{60}$  and  $Cs_6C_{60}$ ,<sup>6</sup>  $Ba_6C_{60}$ ,<sup>10</sup> and  $Rb_6C_{60}$ ,<sup>17</sup> and suggests a  $9.43 \text{ } \text{Å}$  nearest-neighbor separation for the molecules. The atomic coordinates of C1, C2, C3 and Sm are nearly the same as that of  $A_6C_{60}$  (A=K, Rb, Cs, and Ba).<sup>6,10,17</sup>

For the low Sm-doped  $C_{60}$ ,  $Sm_{2.75}C_{60}$  is isostructural with  $Yb_{2.75}C_{60}$ ,<sup>15</sup> and different from the fcc  $A_3C_{60}$  (A=K, Rb).<sup>4</sup> In this structure, the fcc-based subcell of four  $C_{60}$  molecules has

Sm cations occupying all four octahedral (O) interstitial sites but only seven of the eight tetrahedral (T) sites. The unoccupied site alternates between adjacent T sites in each direction, leading to an unit-cell doubling with eight ordered vacancies. The O-site Sm cations are displaced from the centers of their interstices towards the nearest neighbor vacancy, effectively reducing the nearest neighbor coordination of  $C_{60}$  anions around the O-site cation from six to three. Thus, in the unit cell there are three types of  $C_{60}$  molecules. In contrast to the  $RE_{2.75}C_{60}$ , the highly Sm-doped  $Sm_6C_{60}$  is isostructural with  $A_6C_{60}$  (A=K, Rb, Cs, and Ba).<sup>6,10,17</sup> It suggests that further intercalation of Sm into  $C_{60}$  solids leads to disappearance of cation-vacancy ordering and formation of a cation-disordered phase. The number of interstitial sites increases from three per  $C_{60}$  in a faced-centred cubic (fcc) structure to six in the bcc structure. Additionally, the distinction between octahedral and tetrahedral sites is removed in the bcc structure, all interstitial sites becoming equivalent with distorted tetrahedral symmetry. For the  $RE_{2.75}C_{60}$ , the vacancies create three inequivalent types of  $C_{60}$  anions. Each anion rotates about an internal axis to maximize the number of pentagon oriented towards the surrounding cations. In the highly Sm-doped  $Sm_6C_{60}$ , all interstitial sites are filled by six samarium atoms. All  $C_{60}$  balls are equivalent and orientationally uniform, and all the tetrahedral holes are surrounded by two pentagons and two hexagons.

Figure 2 shows room temperature Raman spectrum for the polycrystalline sample of  $Sm_6C_{60}$ . In the spectrum, only one peak of pentagonal pinch  $A_g(2)$  mode is observed, providing an evidence that the sample is a single phase. This agrees fairly well with the x-ray diffraction patterns. It is worthy to note that the Raman spectrum of  $Sm_6C_{60}$  is amazingly similar to that of  $Ba_6C_{60}$ ,<sup>18</sup> suggesting that the electronic states of  $Sm_6C_{60}$  is similar to that of  $Ba_6C_{60}$ . The positions ( $\omega$ ) and halfwidths ( $\gamma$ ) of the Raman modes observed are listed in Table I. For comparison, the lines for pure  $C_{60}$  and  $Ba_6C_{60}$  are included in Table I. The frequencies of the two  $A_g$  derived modes are 505.5 and 1371  $cm^{-1}$ , respectively. Which are different from 498.3 and 1432.8  $cm^{-1}$  observed for the corresponding  $A_g$  modes in  $Sm_{2.75}C_{60}$ .<sup>19</sup> It also provides a direct evidence for an existence of new phase in Sm-doped  $C_{60}$  system. It is seen in table I that the frequencies of the two  $A_g$  modes are nearly the same as those in  $Ba_6C_{60}$ . It suggests that  $C_{60}$  in  $Sm_6C_{60}$  is hexavalent, being in a fair agreement with a simple expectation assuming that Sm cation is divalent. This is consistent with the results of near-edge and extended X-ray absorption fine structure in  $Yb_{2.75}C_{60}$ ,<sup>20</sup> and Raman scattering results of  $Sm_{2.75}C_{60}$ ,<sup>19</sup> in which Sm cation is confirmed to be divalent.

Two theoretical calculations based the local density approximation have shown a strong hybridization between the alkaline-earth-atom states and the  $C_{60}$   $\pi$  states.<sup>21,22</sup> Recent photoemission studies have also indicated the presence of a hybrid band with incomplete charge transfer from alkaline-earth metals to  $C_{60}$ , as a consequence of the competition between covalent  $Ba - C_{60}$  bonding and ionic contribution.<sup>23</sup> The same frequency of the  $A_g(2)$  mode as that in  $Ba_6C_{60}$ , which is known as a sensitive probe for the degree of charge transfer on  $C_{60}$  molecule, indicates that the hybridization between Sm atom and  $C_{60}$  molecules could exist in  $Sm_6C_{60}$ . In fact, the size of the divalent samarium, 1.18 Å, placed at (0.22, 0.5, 0) requires a lattice constant of about 11.5 Å assuming spherically symmetric molecules. The relatively small lattice constant measured also may indicate strong orbital overlap between the neighboring molecules. This hybridization may play an essential role for a larger Raman downshift of the pentagonal pinch  $A_g(2)$  mode than that expected by the simple relation between Raman shift and charge transfer widely observed in  $K_xC_{60}$ .<sup>24,25</sup>

In the table I, the positions and halfwidths were obtained by fitting the experimental data with Lorentzian line shape. It is easily seen that the lowest frequency  $H_g$  modes are splitted into several components. The similar behavior has been observed in single crystal  $K_3C_{60}$  at low temperature<sup>26</sup> and in  $Ba_xC_{60}$  (x=4 and 6).<sup>18</sup>  $H_g(2)$  mode is apparently split into five components in  $Sm_6C_{60}$ . The inset of Fig.2 shows the results of a line-shape analysis for  $H_g(2)$  mode. It suggests that the five-fold degeneracy is completely lift. This splitting of  $H_g(2)$  mode in  $Sm_6C_{60}$  is unexpected since the group theoretical consideration predicts a splitting into two in the space group  $I_{m\bar{3}}(T_5^h)$ . The splitting might suggest a symmetry lowering which is not detected in the x-ray diffraction. This type of disagreement between microscopic spectroscopy and structural analysis was observed in  $Rb_3C_{60}$ <sup>27</sup> and  $Ba_6C_{60}$ .<sup>18</sup> From Table I, we can find that the positions for most of modes are the same, and the similar splitting is observed in  $Sm_6C_{60}$  and  $Ba_6C_{60}$ . This strongly indicates that  $Sm_6C_{60}$  and  $Ba_6C_{60}$  have a similar crystal structure and electronic states.

Figure 3 show the temperature dependence of resistivity for the sample  $Sm_6C_{60}$ . No superconducting transition is observed at the temperature down to 4.2 K. A minimum resistivity appears at about 180 K. The temperature coefficient of resistivity is positive over 180 K, while is negative below 180 K. The data in Fig.3 are fitted by the following formula:

$$\rho = ae^{-bT^{-1/2}} + cT + d \quad (1)$$

where a, b, c, and d are the fitting parameters. It is found that data can be well fitted over the whole temperature range of 4.2-300 K by the formula. The first item in the formula is written according to the granular metal theory, in which the  $\ln\rho$  is proportional to the  $T^{-1/2}$ . The linear-T item is used to fit the metallic behavior at the high temperature. The inset of Fig.3 plots the same data as  $\ln\rho$  vs  $T^{-1/2}$ , and almost shows a linear relation below 180 K. It suggests that the transport is dominated by the granular-metal theory. Stepniak et al. have reported that the thin film samples of  $Rb_xC_{60}$  can be described within the framework of granular metal theory.<sup>28</sup> The sample  $Sm_6C_{60}$  shows a weak localization behavior at low temperature and the ratio  $\rho(4.2K)/\rho(290K)$  is only 1.7. In addition, the transport at low temperature can be explained by the granular metal theory. These results indicate that the sample  $Sm_6C_{60}$  is metallic. This is in apparent contradiction to the insulating electronic structure if the charge complete transfer from the rare-earth divalent Sm atom to  $C_{60}$  molecules could result in the full occupation of the  $t_{1g}$  band. The metallic behavior of  $Sm_6C_{60}$  suggests that there could exist a hybridization between rare-earth Sm  $f$  orbitals and  $C_{60}$   $p$   $\pi$  orbitals, being similar to the case of  $Ba_6C_{60}$ . In the case of  $Ba_6C_{60}$ , the theoretical calculation based on the local-density approximation shows that the hybridization between the Ba atom s states and the  $C_{60}$   $\pi$  states is essential for the metallic electronic structure.<sup>21</sup> In addition, the same Raman shift of the  $A_g(2)$  pinch mode for  $Sm_6C_{60}$  and  $Ba_6C_{60}$  also provides a direct evidence for a hybridization between Sm atoms and  $C_{60}$  molecules. In order to further confirm the hybridization in  $Sm_6C_{60}$ , a theoretical calculation or photoemission study is necessary.

In summary, we synthesized a novel fulleride  $Sm_6C_{60}$ , which was characterized by X-ray diffraction, Raman scattering and resistivity measurement.  $Sm_6C_{60}$  adopts body-centered cubic structure, being similar to that of  $A_6C_{60}$  (A=K, Rb, Ba). Raman spectrum of  $Sm_6C_{60}$  is strikingly similar to that of  $Ba_6C_{60}$ . The same Raman shift of the  $A_g(2)$  pinch mode in  $Sm_6C_{60}$  and  $Ba_6C_{60}$  suggests that Sm is divalent and there exists a hybridization between

rare-earth Sm atom and the  $C_{60}$  molecules, which could be responsible for the metallic behavior of  $Sm_6C_{60}$  observed by resistivity measurement. A weak T-linear metallic behavior is observed down to 180 K, the resistivity data at low temperature can be explained by the granular-metal theory.

#### **ACKNOWLEDGMENTS**

This work is supported by Grant from Natural Science Foundation of China.

## REFERENCES

- <sup>1</sup> R.C. Haddon, A.F. Hebard, M.J. Rosseinsky, D.W. Murphy, S.J. Duclos, K.B. Lyons, B. Miller, J.M. Rosamilia, R.M. Fleming, A.R. Kortan, S.H. Glarum, A.V. Makhija, A.J. Muller, R.H. Eick, S.M. Zahurak, R. Tycko, G. Dabbagh, and F.A. Thiel, *Nature* **350**, 320(1991).
- <sup>2</sup> P.W. Stephens, G. Bortel, G. Faigel, M. Tegze, A. Janossy, S. Pekker, G. Oszlanyki, L. Forro, *Nature* **370**, 636(1994).
- <sup>3</sup> A.F. Hebard, M.J. Rosseinsky, R.C. Haddon, D.W. Murphy, S.H. Glarum, T.T.M. Palstra, A.P. Ramirez, and A.R. Kortan, *Nature* **350**, 600(1991).
- <sup>4</sup> P.W. Stephens, L. Mihaly, P.L. Lee, R.L. Wheten, S.M. Huang, R.B. Kaner, F. Diederich, and K. Holczer, *Nature* **351**, 632(1991).
- <sup>5</sup> R.M. Fleming, M.J. Rosseinsky, A.P. Ramirez, D.W. Murphy, J.C. Tully, R.C. Haddon, T. Siegrist, R. Tycko, H. Glarum, P. Marsh, G. Dabbagh, S.M. Zahurak, A.V. Makhija, and C. Hampton, *Nature* **352**, 701(1991).
- <sup>6</sup> O. Zhou, J.E. Fisher, N. Coustel, S. Kycia, Q. Zhu, A.R. McGhie, W.J. Romanow, J.P.Jr. McCauley, A.B. Smith, and D.E. Cox, *Nature* **351**, 462(1991).
- <sup>7</sup> R.M. Fleming, A.P. Ramirez, M.J. Rosseinsky, D.W. Murphy, R.C. Haddon, S.M. Zahurak, and A.V. Makhija, *Nature* **352**, 787(1991).
- <sup>8</sup> T. Yildirim, L. Barbedette, J.E. Fisher, C.L. Lin, J. Robbert, P. Petit, and T.T.M. Palstra, *Phys. Rev. Lett.* **77**, 167(1996).
- <sup>9</sup> A.R. Kortan, N. Kopylov, S. Glarum, E.M. Gyorgy, A.P. Ramirez, R.M. Fleming, F.A. Thiel, and R.C. Haddon, *Nature* **355**, 529(1992).
- <sup>10</sup> A.R. Kortan, N. Kopylov, S. Glarum, E.M. Gyorgy, A.P. Ramirez, R.M. Fleming, O. Zhou, F.A. Thiel, P.L. Trevor, and R.C. Haddon, *Nature* **360**, 566(1992).
- <sup>11</sup> A.R. Kortan, N. Kopylov, E. Özdás, A.P. Ramirez, R.M. Fleming, and R.C. Haddon, *Chem. Phys. Lett.* **233**, 501(1994).
- <sup>12</sup> A.R. Kortan, N. Kopylov, R.M. Fleming, O. Zhou, F.A. Thiel, and R.C. Haddon, *Phys. Rev. B* **47**, 13070(1993).
- <sup>13</sup> M. Baenitz, M. Heinze, K. Lüders, H. Werner, R. Schögl, M. Weiden, G. Sparn, and F. Steglich, *Solid State Commun.* **96**, 539(1995).
- <sup>14</sup> E. Özdás, A.R. Kortan, N. Kopylov, A.R. Ramirez, T. Siegrist, K.M. Rabe, H.E. Bair, S. Schuppler, and P.H. Citrin, *Nature* **375**, 126(1995).
- <sup>15</sup> X.H. Chen and G. Roth, *Phys. Rev. B* **52**, 15534(1995).
- <sup>16</sup> K.M. Rabe and P.H. Citrin, *Phys. Rev. B* **58**, 551(1998).
- <sup>17</sup> Q. Zhu, O. Zhou, N. Coustel, G.B.M. Vaughan, J.P.Jr. McCauley, W.J. Romanov, J.E. Fisher, and A.B. Smith, *Science* **254**, 545(1991).
- <sup>18</sup> X.H. Chen, S. Taga, and Y. Iwasa, *Phys. Rev. B* (to be published).
- <sup>19</sup> X.H. Chen, T. Takenobu, T. Muro, H. Fudo, and Y. Iwasa, submitted to *Phys. Rev. B*
- <sup>20</sup> P.H. Citrin, E. Özdás, S. Schuppler, A.R. Kortan, and K.B. Lyons *Phys. Rev. B* **56**, 5213(1997).
- <sup>21</sup> S. Saito and A. Oshiyama, *Phys. Rev. Lett.* **71**, 121(1993).
- <sup>22</sup> S.C. Erwin and M.R. Pederson, *Phys. Rev. B* **47**, 8249(1993).
- <sup>23</sup> Th. Schedel-Niedrig, M.C. Böhm, H. Werner, J. Schulte, and R. Schögl, *Phys. Rev. B* **55**, 13542(1997).

- <sup>24</sup> S.J. Duclos, R.C. Haddon, S.H. Glarum, A.F. Hebard, and K.B. Lyons, *Science* **254**, 1625(1991).
- <sup>25</sup> H. Kuzmany, M. Matus, B.Burger, and J. Winter, *Adv. Mater.* **6**, 731(1994).
- <sup>26</sup> J. Winter and H.Kuzmany, *Phys. Rev. B* **53**, 655(1996).
- <sup>27</sup> R.E. Walstedt, D.W. Murphy, and M.J. Rosseinsky, *Nature* **362**, 611(1993).
- <sup>28</sup> F. Stepniak, P.J. Benning, D.M. Poirier, and J. Weaver, *Phys. Rev. B* **48**, 1899(1993).

TABLES

TABLE I. Positions and linewidths (in parentheses) for the Raman modes in  $C_{60}$  and  $Ba_6C_{60}$

$I_h$ mode	$C_{60}$ $\omega$ ( $\gamma$ ) ( $cm^{-1}$ )	$Ba_6C_{60}$ $\omega$ ( $\gamma$ ) ( $cm^{-1}$ )	$Sm_6C_{60}$ $\omega$ ( $\gamma$ ) ( $cm^{-1}$ )
$A_g(1)$	493	506.5 ( 5.0 )	505.5 ( 3.3 )
$A_g(2)$	1469	1372.5 ( 12.1 )	1371.0 ( 7.0 )
$H_g(1)$	270	274.5 ( 5.2 )	263.4 ( 7.8 )
		281.8 ( 2.6 )	280.0 ( 13.9 )
			291.8 ( 3.7 )
$H_g(2)$	431	385.6 ( 4.4 )	367.2 ( 7.1 )
		405.8 ( 2.2 )	391.6 ( 5.1 )
		415.6 ( 2.4 )	400.8 ( 4.1 )
		428 ( 16.8 )	415.9 ( 28.2 )
		438.8 ( 2.8 )	426.8 ( 6.4 )
$H_g(3)$	709	585.2 ( 4.8 )	587.5 ( 28.0 )
		602.1 ( 5.2 )	603.2 ( 10.8 )
		622.3 ( 3.7 )	638.0 ( 32.0 )
		651.8 ( 12.0 )	
$H_g(4)$	773	732.5 ( 8.5 )	740.0 ( 9.0 )
$H_g(5)$	1099	1082 ( 6.0 )	1084.0 ( 12.0 )
			1110.2 ( 10.8 )
$H_g(6)$	1248	1224 ( 26 )	1210.5 ( 6.5 )
			1227.2 ( 10.3 )
$H_g(7)$	1426		
$H_g(8)$	1573	1437 ( 25.0 )	1440.5 ( 20.2 )



## FIGURE CAPTIONS

Figure 1:

X-ray diffraction pattern of the sample  $Sm_6C_{60}$  collected with synchrotron radiation. The synchrotron beam was monochromatized to 0.8500 Å. The crosses are experimental points and the solid line is a Rietveld fit to the model  $Sm_6C_{60}$  in the space group  $I_{m\bar{3}}$ . The allowed reflection positions are denoted by ticks.

Figure 2:

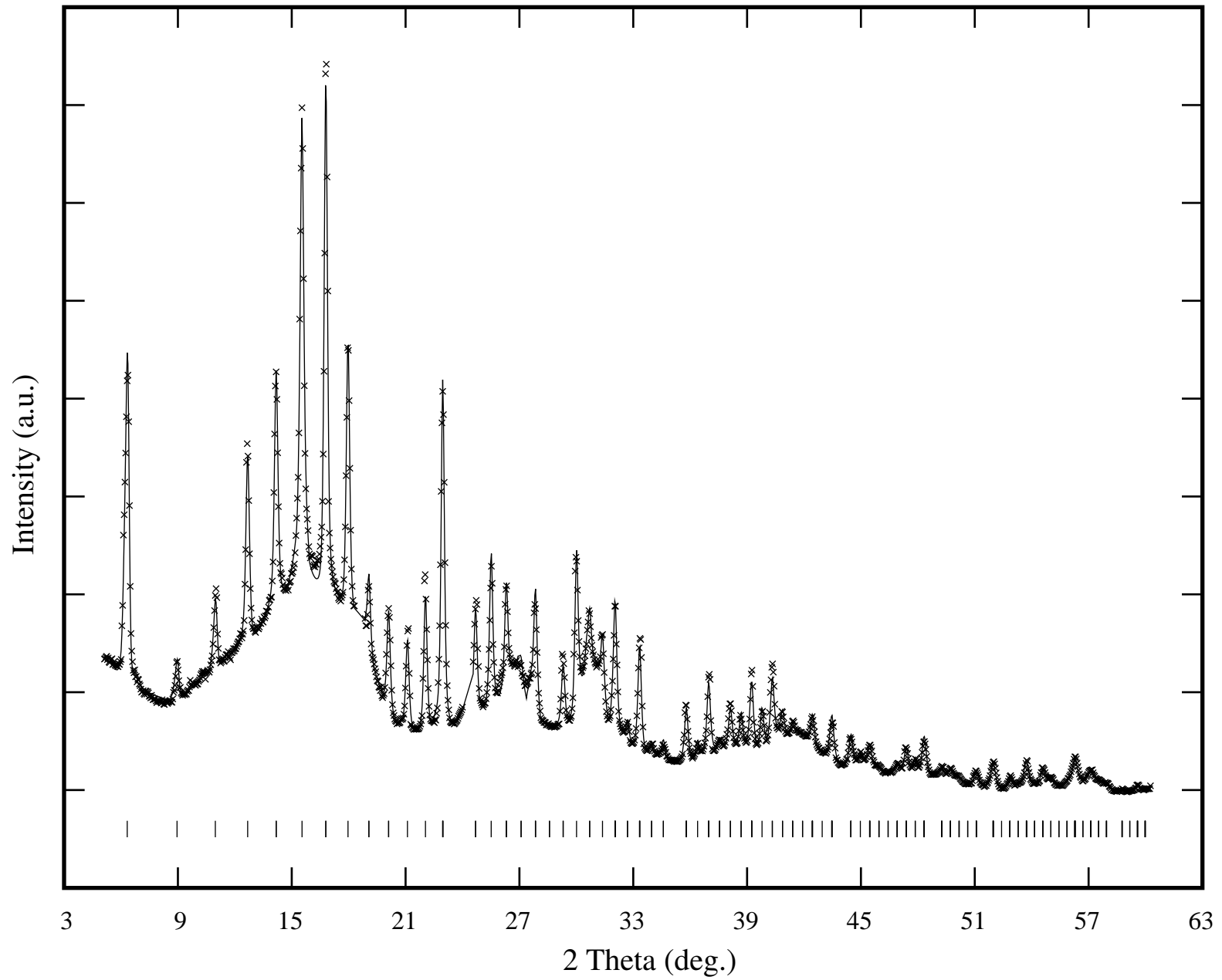
Room temperature Raman spectrum of  $Sm_6C_{60}$ . The results of a line-shape analysis for  $H_g(2)$  mode are shown (inset). The dash lines are computer fits for the individual components, which add up to the full line on the top of the experimental results.

Figure 3:

The temperature dependence of resistivity for the polycrystalline  $Sm_6C_{60}$ . Inset plots the same data as  $\ln\rho$  vs  $T^{-1/2}$ . A linear relation would be expected if the charge transport did follow the granular-metal theory.

**Fig.1**

**X.H. Chen et al.**



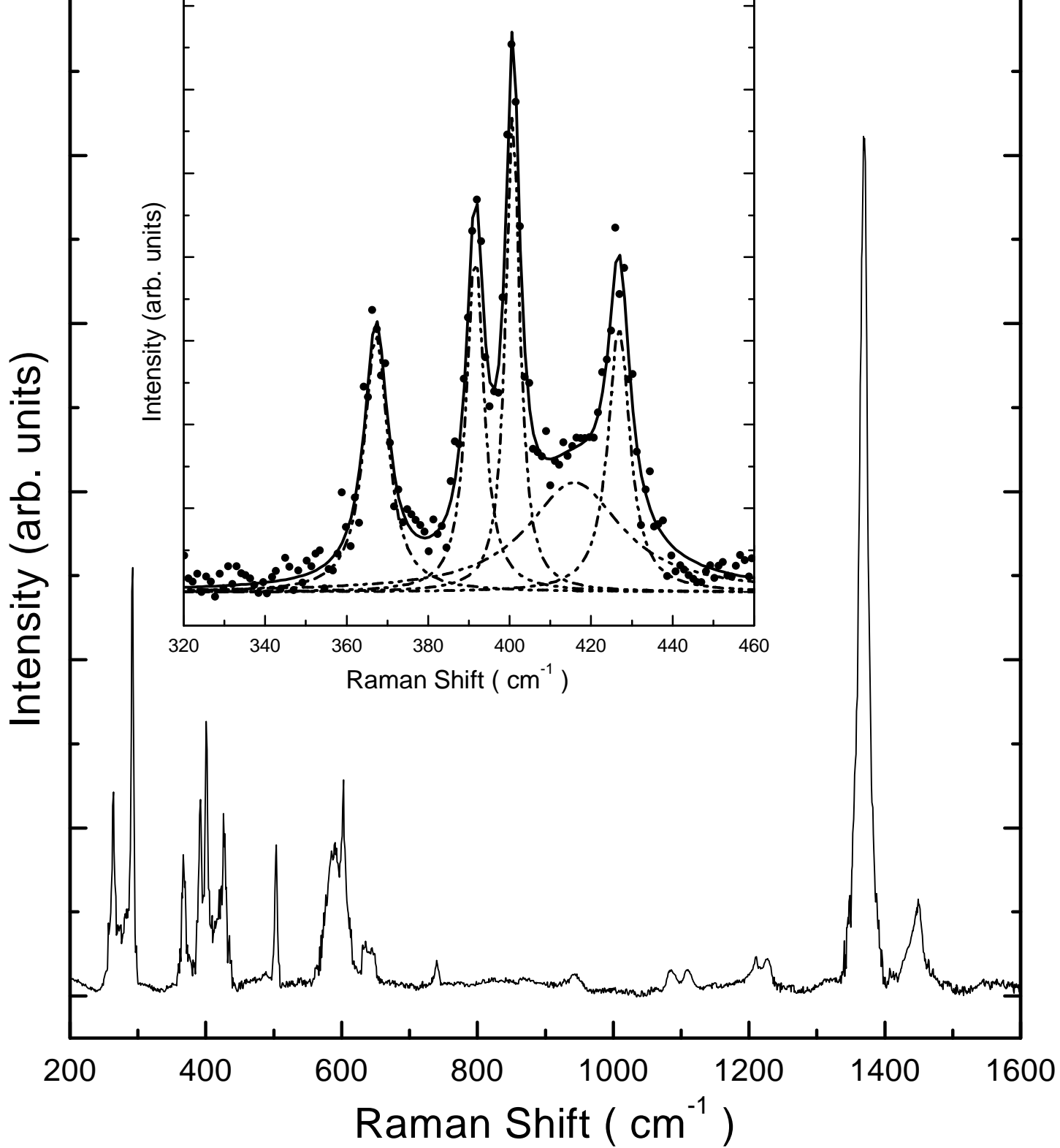


Fig.2

X.H. Chen et al.

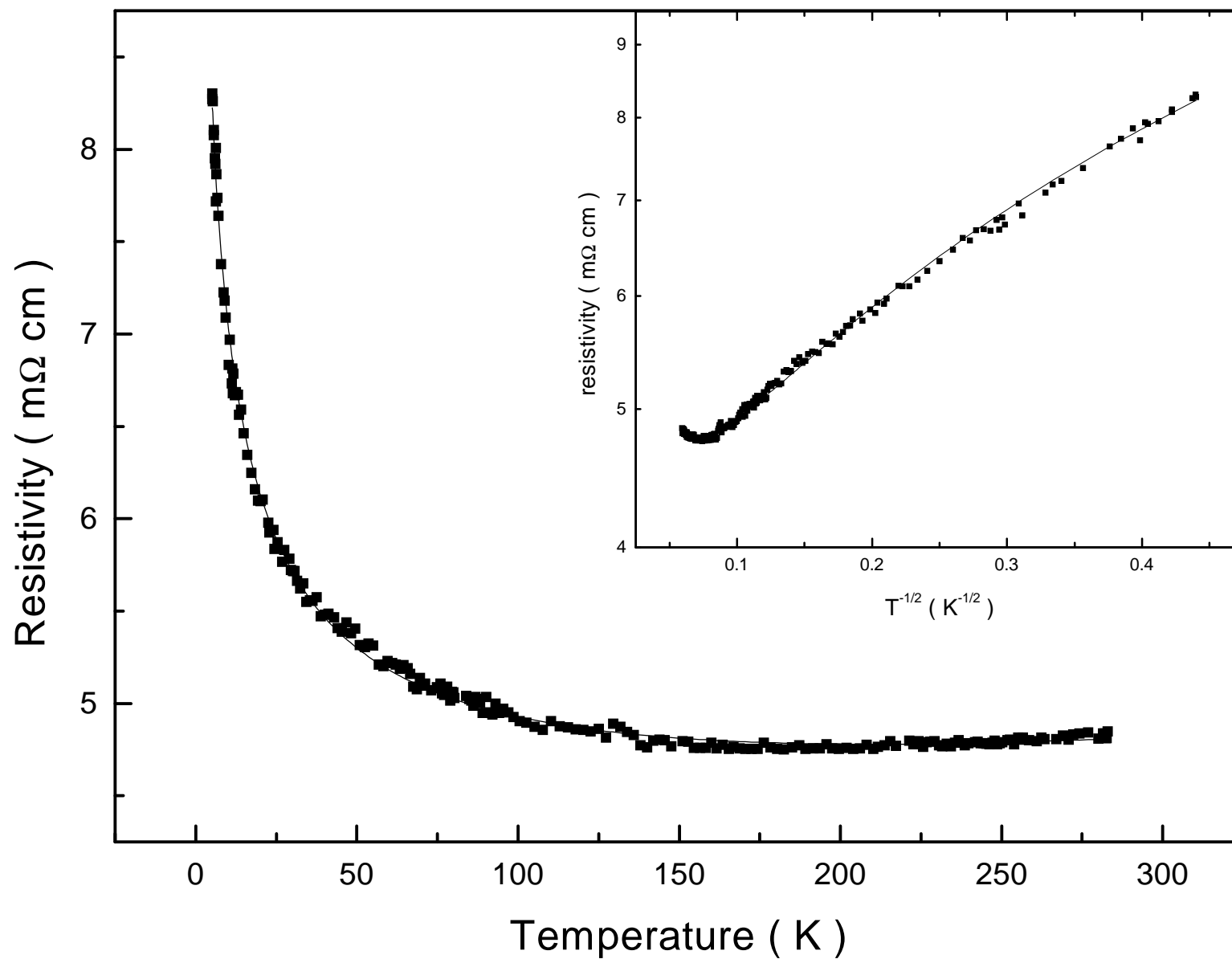


Fig.3

X.H. Chen et al.